

# Co-seismic Landslide Inventory and Susceptibility Mapping in the 2008 Wenchuan Earthquake Disaster Area, China

LI Wei-le<sup>1,2\*</sup>, HUANG Run-qiu<sup>1</sup>, TANG Chuan<sup>1</sup>, XU Qiang<sup>1</sup>, Cees van WESTEN<sup>2</sup>

*1 State key Laboratory of Geohazard Prevention and Geoenvironment Protection, Chengdu University of Technology, Chengdu 610059, China*

*2 Faculty of Geoinformation Science and Earth Observation (ITC), University of Twente, Enschede 7500AA, The Netherlands*

*\*Corresponding author, e-mail: whylw01@163.com*

© Science Press and Institute of Mountain Hazards and Environment, CAS and Springer-Verlag Berlin Heidelberg 2013

**Abstract:** The Ms 8.0 May 12, 2008 Wenchuan earthquake triggered tens of thousands of landslides. The widespread landslides have caused serious casualties and property losses, and posed a great threat to post-earthquake reconstruction. A spatial database, inventoried 43,842 landslides with a total area of 632 km<sup>2</sup>, was developed by interpretation of multi-resolution remote sensing images. The landslides can be classified into three categories: swallow, disrupted slides and falls; deep-seated slides and falls, and rock avalanches. The correlation between landslides distribution and the influencing parameters including distance from co-seismic fault, lithology, slope gradient, elevation, peak ground acceleration (PGA) and distance from drainage were analyzed. The distance from co-seismic fault was the most significant parameter followed by slope gradient and PGA was the least significant one. A logistic regression model combined with bivariate statistical analysis (BSA) was adopted for landslide susceptibility mapping. The study area was classified into five categories of landslide susceptibility: very low, low, medium, high and very high. 92.0% of the study area belongs to low and very low categories with corresponding 9.0% of the total inventoried landslides. Medium susceptible zones make up 4.2% of the area with 17.7% of the total landslides. The rest of the area was classified into high and very high categories, which makes up 3.9% of the area with corresponding 73.3% of the total landslides. Although the susceptibility map can reveal the likelihood of future landslides and debris flows, and it is helpful for the rebuilding process and future zoning issues.

**Keywords:** Wenchuan Earthquake; Landslide; Inventory; Susceptibility mapping; Logistic regression

## Introduction

At 2:28 p.m. on May 12, 2008 (Beijing time), a catastrophic earthquake of Ms 8.0 struck the eastern edge of the Tibetan plateau (Tom et al. 2008). The epicenter with a focal depth of 14 km was in Yingxiu town, located in Wenchuan county, which is part of Sichuan province, in the southwest of China (31.02°N and 103.37°E) (Dai et al. 2011). The earthquake was one of the deadliest disaster events in the history of China, with about 70,000 fatalities and 18,000 listed as missing (Dai et al. 2010). It triggered tens of thousands of landslides over a broad region in the Longmen Mountain region and one third of the casualties were caused by co-seismic landslides (Wang et al. 2009). The estimated volume of materials displaced by the co-seismic landslides ranges between 5 and 15 km<sup>3</sup> (Parker et al. 2011), which will have a long-term influence on the stability of slopes in the earthquake disaster area.

Although it caused heavy losses, the Wenchuan earthquake provided a rare opportunity for geologists to carry out detailed research on co-seismic landslides. Huang and Li (2009a, 2009b) carried out a rapid landslide inventory by field investigation and interpretation of aerial photos and satellite images after the quake, and mapped 11,308 landslides. Yin et al. (2009) reported that

---

**Received:** 28 July 2012  
**Accepted:** 15 April 2013

more than 15,000 landslides were triggered by the Wenchuan earthquake and analyzed the mechanism of some typical landslides. Qi et al. (2010) mapped 13,085 landslides with a total area of 418.85 km<sup>2</sup> and analyzed the correlation between the landslide distribution and geological factors such as faults, lithology and topography. Using higher resolution aerial photos and remote sensing images covering almost the entire disaster area, Dai et al. (2011) made an inventory of about 56,000 landslides, with a total area of 811 km<sup>2</sup>. They mapped the landslides as polygons, without differentiating between scarp areas and accumulation areas, and the relation with distance from the major surface rupture, distance from the epicenter, seismic intensity, slope angle, slope aspect, elevation, and lithology. A similar work was carried out by Gorum et al. (2011), who mapped 60,000 landslides as points using a large set of satellite images and their distribution pattern was analyzed with the seismic and geology parameters. Clearly, from the above results it is very difficult to obtain a so-called complete landslide inventory for a single event such as the Wenchuan earthquake. Many factors play a role in determining the completeness of the inventory, such as the differences in the area mapped, the coverage, resolution and date of the images used in the inventory mapping, the skills of the interpreters, the time spent on making the inventory, the method of image interpretation (monoscopic/stereoscopic, single date or using pre- and post earthquake comparisons) and the mapping method (point or polygons, differentiation between types, and accumulation/erosional areas) (Soeters and Van Westen 1996; Qi et al. 2012; Guzzetti et al. 2012).

Landslide is one of the most damaging natural hazards, their activity is difficult to predict, but they can be evaluated by susceptibility analysis (Varnes 1984). A landslide susceptibility map is intended to provide planners and local residents with information of potentially dangerous regions and it is a helpful tool for land management and infrastructure reconstruction after an earthquake. The reliability of landslide susceptibility maps depends mostly on the amount and quality of the data source, the assessment scale and the analysis methodology (Ayalew and Yamagishi 2005). Many multivariate statistical approaches exist, but

logistic regression is a widely used statistical approach (Soeters and Westen 1996; Aleotti and Chowdhury 1999; Ayalew and Yamagishi 2005; Su et al. 2010; Dong et al. 2011; Xu et al. 2012a). Das et al. (2010) compared the logistic regression method for landslide susceptibility mapping with the geotechnical-based slope stability probability classification (SSPC) methodology in a landslide-prone national highway road section in the northern Indian Himalayas. Bai et al. (2010) extended the application of logistic regression approaches to use all continuous variables, and the landslide density was used to transform these nominal variables to numeric variable. Das et al. (2012) presented a Bayesian logistic regression (BLR) for landslide susceptibility mapping along road corridors in the Indian Himalayas and the result indicated BLR performs better in posterior parameter estimation in general and the uncertainty estimation in particular. Aykut (2012) carried out a comparison of landslide susceptibility maps produced by logistic regression, multi-criteria decision, and likelihood ratio methods in western Turkey, and found that logistic regression was the most accurate method. Das et al. (2012) presented a Bayesian logistic regression (BLR) for landslide susceptibility mapping along road corridors in the Indian Himalayas and the result indicated BLR performs better in posterior parameter estimation in general and the uncertainty estimation in particular. Xu et al. (2012a) compared bivariate statistics (BS), logistic regression (LR), artificial neural networks (ANN), and three types of support vector machine (SVM) models for susceptibility mapping of the Wenchuan earthquake triggered landslides in the watershed of the Fujiang River. The result also indicated that the LR model provided the highest success rate and the highest prediction rate.

Many researchers have produced landslide susceptibility maps for parts of the Wenchuan earthquake affected area, mostly based on statistical models that correlate the co-seismic landslide distribution with a number of tectonic, geological and topographical factors. Tang et al. (2009) carried out an emergency assessment of co-seismic landslide susceptibility in Qingchuan County, which is one of the 39 worst-hit county in Sichuan province. Su et al. (2010) also chose Qingchuan County as a case study of landslide

susceptibility mapping with LR model. Lithology, distance from major fault, slope angle, profile curvature, and elevation were selected as affecting parameters in their model. The prediction ability of different susceptibility mapping models such as BS, LR, ANN, SVM, Weight of Evidence (WE) was tested by Xu et al. (2012 a) in Fujiang River, Qingshui River and Jianjiang River watershed. Song et al. (2012) assessed the co-seismic landslide susceptibility of Beichuan region using Bayesian network (BN) model. Many case studies of a relatively small region such as a watershed or a county have been carried out (Su et al. 2010, Xu et al. 2012 a,b,c), but the susceptibility mapping of the whole meizo-seismal area is rare. This study presents the inventory of the co-seismic landslides by imagery interpretation and the GIS-based logistic regression model for susceptibility mapping for a region of 37 hardest-hit counties, almost covering the whole Wenchuan earthquake area.

### 1 Study Area

The Wenchuan earthquake occurred in the Longmenshan fault region at the eastern margin of the Qinghai-Tibetan Plateau, adjacent to the Sichuan Basin. The Longmenshan fault zone is one of the zones in the world with the steepest slope-gradients. Across the Longmenshan range, the elevation rises sharply from 500 m in the Sichuan Basin to 4,000-6,000 m on the Tibetan Plateau over a distance of 100 km. The structure of the northeast-trending Longmenshan Fault belt was formed as an intercontinental transfer fault, with a length of approximately 500 km, and is composed of three major thrusts, including the Maoxian – Wenchuan fault, the Yingxiu – Beichuan fault and the Jianguyou – Guanxian fault (Hang and Li 2009a, b). The earthquake ruptured both the Yingxiu-Beichuan (about 240 km long) and Jianguyou-Guanxian faults (72 km long) (Figure 1), while the magnitude and proportion of dextral strike-slip

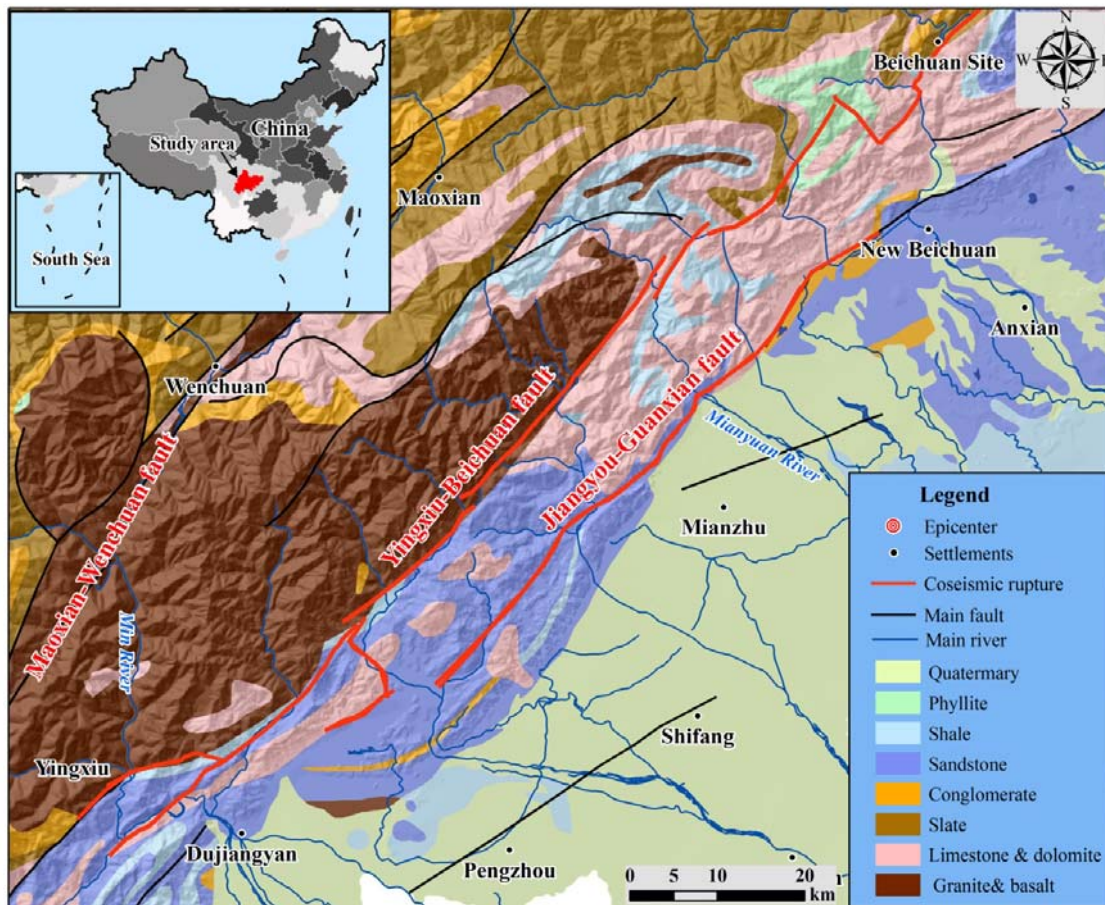


**Figure 1** Geological and tectonic settings of the Wenchuan earthquake area adapted from 1:500,000 geologic maps

and thrust dip-slip fault displacement varied significantly along the rupture trace, with two distinct zones of concentrated slip and moment release near Yingxiu and Beichuan Site (Parker et al. 2011). The maximum thrust slip was about 10.8 m, and the maximum right-lateral displacement was about 8.8 m (Dai et al. 2011). The rocks in the Wenchuan earthquake area range from Mesozoic, Jurassic, Cretaceous, Paleozoic, to Precambrian in age and consist mainly of granite, basalt, dolomite, limestone, sandstone, slate, shale, phyllite, etc. (Figure 1).

The basic unit in the management of landslide risk in China is county, and most of the landslide susceptibility mapping researches take a county as the basic unit. After the emergency investigation, 39 counties in Sichuan province were identified as most seriously affected. This study analyzed these 37 counties with a total area of 93,000 km<sup>2</sup>, among which the top ten most destroyed counties are: Wenchuan, Beichuan, Mianzhu, Shifang, Qingchuan, Maoxian, Anxian, Dujiangyan, Pingwu and Pengzhou (Figure 2).

## 2 Landslide Inventory

### 2.1 Data and methodology

After the main shock of the Wenchuan Earthquake, Chinese government immediately organized teams of geologists to conduct the co-seismic landslide investigation as a basis for the planning of transitional resettlement sites and reconstruction planning. More than 15,000 landslides were recorded by the emergency field investigation (Yin et al. 2009). Due to the inaccessibility and the large area of the affected region, it was impossible to carry out detailed field investigation in the whole disaster area. Thus, most of the researches on generating landslide inventories of the co-seismic landslides were carried out by means of interpretation of aerial photos and multi-resolution satellite images, such as IKONOS, Cartosat-1 images, ALOS image and ASTER images (Figure 2). The aerial photos and satellite images were geometrically corrected using ground-control points selected from the 1:50,000

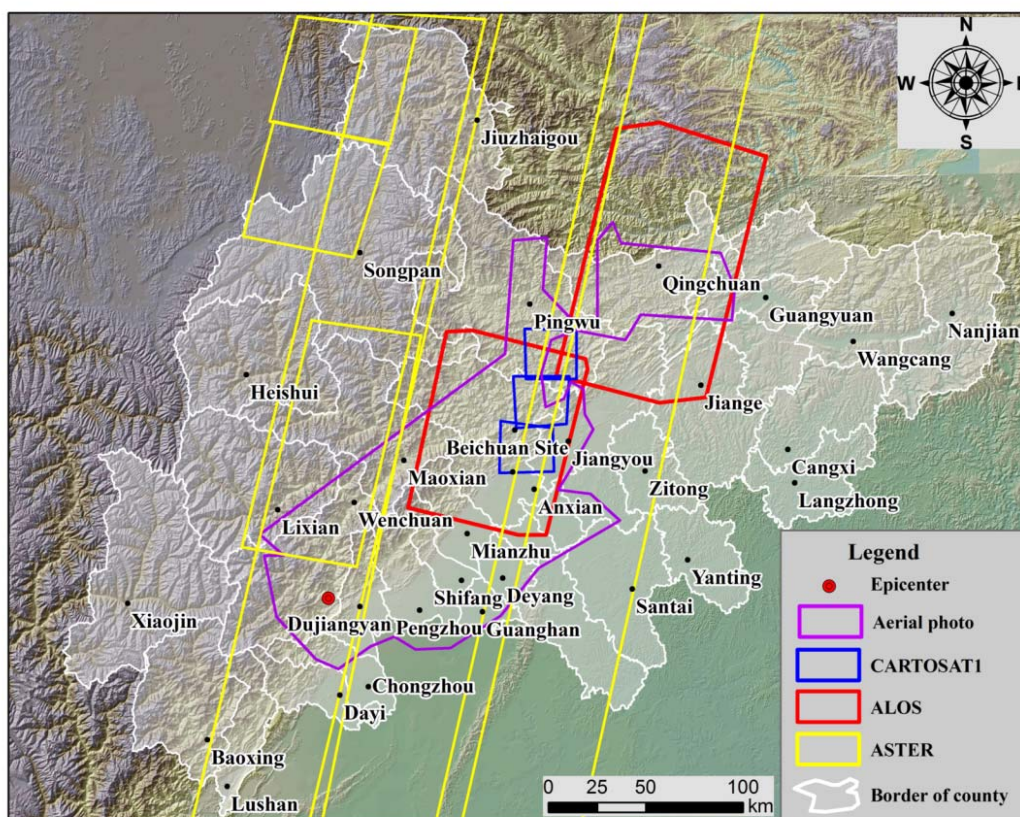


**Figure 2** The spatial coverage of the satellite images and aerial photos of the post-earthquake

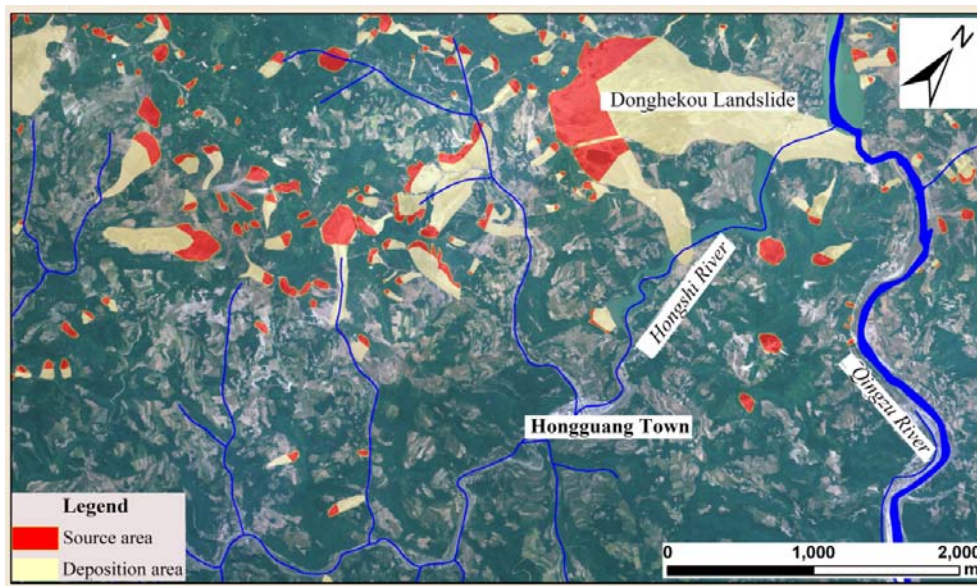


**Figure 3** Landslides distribution in Hongshi River basin, Qingchuan County by interactive visual interpretation of aerial photos

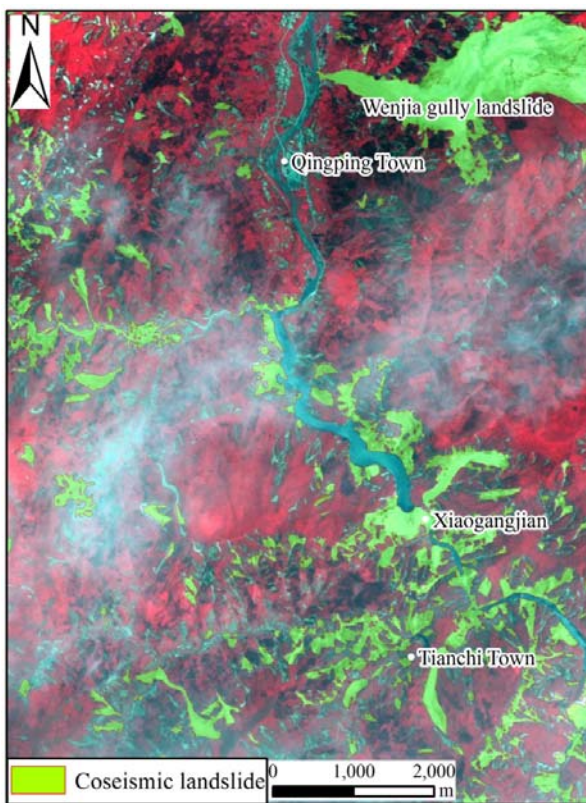


**Figure 4** Landslides in the Mianzhu River basin, Mianzhu County by automatic classification of ALOS images

topographical maps. The images covered the most but not all of the study area. So only the landslides in the images covered areas can be inventoried.

Landslide interpretation was conducted with ArcGIS 9.3, ERDAS Imagine 9.0 and ENVI 4.5.

The co-seismic landslides caused the dramatic changes of surface vegetation, which could be easily identified in the aerial photos and satellite images. However, it has been proven much more difficult to map the individual landslides, and separate them into the erosional and accumulation areas, as in many cases these were difficult to distinguish on the images. In this study, we mapped the landslides as individual polygons, separating the source areas and depositional area (Figure 3). This was, however, much more difficult using the lower resolution images such as, ALOS or ASTER images (Figure 4). Since the landslide sources represent locations where the landslides were initiated, only the source areas may be used to train the susceptibility model. Thus we also put a point in the middle of each landslide's source area for susceptibility analysis. In this study we mapped a total of 43,842 landslides with a total area of 632 km<sup>2</sup> (Figure 5).

## 2.2 Landslide types

Huang et al. (2011) divided the landslides triggered by the Wenchuan earthquake into 5 main categories and 14 subdivisions in terms of the failure mechanisms and dynamic features based on field investigation. With the remote sensing data,

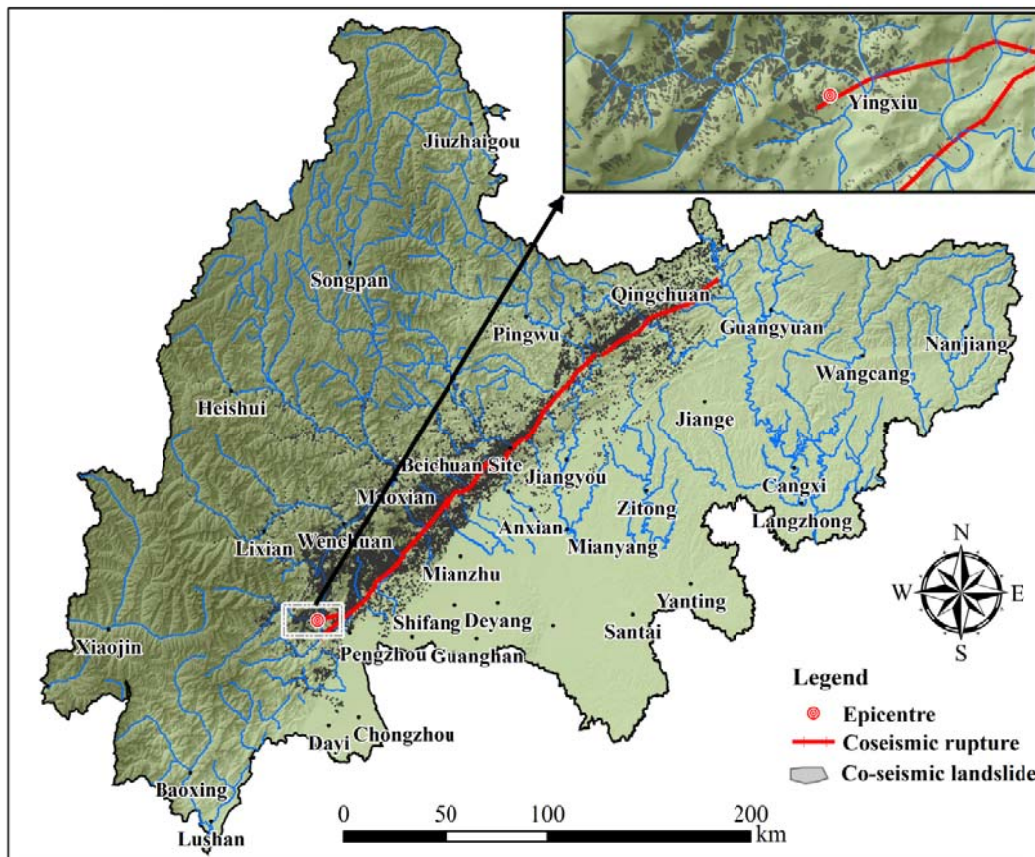


**Figure 5** Distribution of landslide triggered by the Wenchuan earthquake



**Figure 6** A typical shallow landslide in Mianyuan River basin, Mianzhu County, controlled by structural geology



**Figure 7** A deep seated landslide (Xiaogangjian landslide) blocked the Mianyuan River in Mianzhu County

we classified the landslides triggered by the Wenchuan earthquake into three major categories: shallow, disrupted slides and falls (Figure 6); deep-seated landslides (Figure 7) and rock avalanches with long run-out and high speed (Figure 8). The first type of landslides, which can also be induced by relatively weak shaking, were widespread throughout the study area. Deep seated and large scale landslides caused by stronger shaking were

mainly distributed within a distance of 5 km from the Yingxiu-Beichuan fault rupture (Xu et al. 2011). And the strongest shaking was caused by long run-out and high speed rock avalanches which were located very close to the seismic fault. The source areas of these landslides are generally located at higher elevations, and these landslides possess large volumes and potential energy, which could turn into kinetic energy in the sliding process,

accounting for their high speed and large run-out distance. The landslide with the longest run-out was the Wenjia gully rock avalanche (Figure 8) near Qingping Town, in Mianzhu County, with a run-out of 4,000 m and an estimated volume of  $5.0 \times 10^7 \text{ m}^3$  (Huang et al. 2008).

### 3 Logistic Regression (LR) Model

#### 3.1 Principle of LR model

LR can be used to establish a multivariate relation between a dependent and several independent variables, in which a result measured with dichotomous variables such as 0 and 1 or true and false, is determined from the independent variables (Ayalew and Yamagishi 2005). In the case of landslide susceptibility mapping, the goal of LR would be to find the best fitting model to describe the relationship between the presence or absence of landslides and a set of independent parameters such as slope gradient, elevation, slope aspect and rock types (Chen and Wang 2007). The model can be written in the simplest form as:

$$P = 1 / (1 + e^{-Y}) \quad (1)$$

where  $P$  is the estimated probability of landslide occurrence, while  $Y$  can be modeled by regression equation as below:

$$Y = \ln (P / (1 - P)) = C_0 + C_1 X_1 + C_2 X_2 + \dots + C_n X_n \quad (2)$$

where  $C_0$  is the intercept of the model,  $n$  is the number of independent parameters, and  $C_1, C_2, \dots, C_n$  are coefficients, which measure the contribution of independent factors ( $X_1, X_2, \dots, X_n$ ) to the variations in  $Y$  (Ayalew and Yamagishi 2005).

Assume that we obtain a sample of  $m$  observations ( $X_j, Y_j$ ),  $j = 1, 2, \dots, m$ ,  $X_j = (x_{1j}, x_{2j}, \dots, x_{nj})$ , then  $Y_j$  is either 1 or 0,  $Y_j = 1$  for a landslide

event, and  $Y_j = 0$  for a non-landslide event. By fitting the multiple logistic regression model using the sample observations, we can estimate the coefficients  $C_i, i = 0, 1, \dots, n$ .

#### 3.2 Analytical approaches

The independent variables are always in different measuring scales, so the first step before the main statistical analysis is to make sure that data have been normalized. In the application for landslide susceptibility mapping, the common solution is to create layers of binary values for each class of an independent parameter (Ayalew and Yamagishi 2005). However, if there are many independent parameters, it would produce a long regression equation and it might also be difficult to understand statistical results and evaluate the role of each independent variable in the final model (Ayalew and Yamagishi 2005). To simplify the interpretation of the resulting LR model, it was combined with bivariate statistical analysis (BSA) in this study, and regression was conducted among the selected most important parameters. A detailed description of the approach to combine LR with BSA is available in Ayalew and Yamagishi (2005).

Because some independent parameters are continuous variables such as slope gradient and elevation, they should be reclassified. Classification of these data layers were primarily guided by the information contained in the landslide inventory and knowledge from previous studies (Chen and Wang 2007). Then the reclassified parameter maps are compared with the point inventory map landslides to calculate each class value on the basis of BSA (Ayalew and Yamagishi 2005). The class value of each data layer was calculated by Equation (2). Firstly, the density of landslide points in each class of a certain parameter was calculated. Then

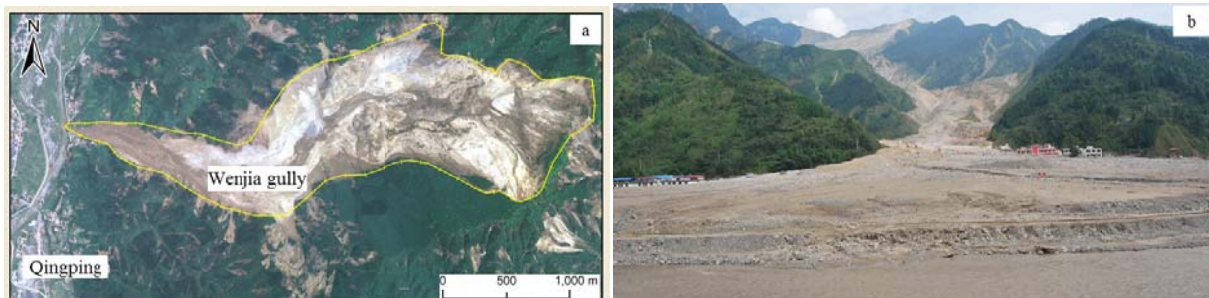


**Figure 8** The longest runout landslide -Wenjia gully rock avalanche in Qingping Town, Mianzhu County. (a)Aerial photo taken on May 23, 2008 after the earthquake;(b)Photo taken on August 22, 2010 after a major debris flow event

these densities were added and each density was divided by the total sum to obtain the value for each class (Table 1).

$$C_{ij} = D_{ij} / \sum D_{ij} \quad (3)$$

where  $C_{ij}$  is the value of each class,  $D_{ij}$  is the density of landslide points in each class,  $\sum D_{ij}$  is the sum of the density of landslide points in each class).

#### 4 Influencing Parameters of Landslides

The most important process in landslide susceptibility mapping is to analyze the link between landslide influencing parameters and the distribution of historical landslides. The selection of influencing factors for landslides susceptibility depends on the assessment scale, the landslide type, the failure mechanisms and the main causes of landslides. A parameter system for susceptibility mapping in different scales including 14 environmental factors and 4 triggering factors was suggested by Westen et al. (2008). There are neither universal criteria nor guidelines for the selection of landslide influencing factors, the general consensus is that any independent variable must be operational, complete, measurable and non-redundant (Ayalew and Yamagishi 2005).

Based on our earlier researches (Huang and Li 2009a, b), 7 major influencing parameters including PGA (as triggering factor), distance from co-seismic fault, lithology, slope gradient, elevation, distance from drainage and slope aspect were prepared and analyzed with the mapped landslides. The independent parameters are all prepared in ARC/INFO GRID format with 50 m cell size (Figure 9).

##### 4.1 PGA

The strong ground motion which cause short lived disturbances in the balance of forces within hill slopes is the main reason for slope failure, and co-seismic landslide was directly induced by strong ground motion (Youd and Perkins 1978; Keefer 1984). PGA is simply the amplitude of the largest peak acceleration recorded on an accelerogram at a site during a particular earthquake. It is often used as a parameter to describe strong ground motion (Douglas 2003). The PGA data in this study was downloaded from USGS's website, which was

**Table 1** Class value of each influencing parameters

Factors	Classes	Density	CV(%)	
Peak ground acceleration (g)	<0.2	0.00558	0.152	
	0.2-0.4	0.08403	2.286	
	0.4-0.6	0.29759	8.094	
	0.6-0.8	0.90000	24.479	
	0.8-1.0	1.66919	45.401	
	>1.0	0.72018	19.588	
Elevation (m)	<600	0.00775	0.404	
	600-1,000	0.18961	9.889	
	1,000-1,500	0.52903	27.591	
	1,500-2,000	0.54826	28.594	
	2,000-2,500	0.39871	20.794	
	2,500-3,000	0.19489	10.164	
	3,000-3,500	0.04058	2.116	
	>3,500	0.00857	0.447	
Distance from fault (km)	HW	0-5	2.527176	26.643
		5-10	1.401698	14.777
		10-15	1.056837	11.142
		15-20	0.680498	7.174
		20-25	0.526754	5.553
		25-30	0.632465	6.668
		>30	0.040516	0.427
	F	0-5	1.104087	11.640
		5-10	0.720373	7.594
		10-15	0.388042	4.091
		15-20	0.186476	1.966
		20-25	0.130127	1.371
		25-30	0.086647	0.913
		>30	0.003384	0.035
Lithology	igneous rock	0.67461	28.939	
	carbonate rock	0.30727	13.181	
	sandstone	0.07201	3.089	
	meta-sandstone	0.05643	2.421	
	slate	0.29242	12.544	
	mudstone	0.08685	3.726	
	shale	0.25504	10.940	
	phyllite	0.57223	24.547	
	soil	0.01432	0.614	
Distance from drainage (m)	0-100	0.25609	13.632	
	100-200	0.35622	18.961	
	200-300	0.44182	23.518	
	300-400	0.36797	19.587	
	400-500	0.29821	15.873	
	>500	0.15835	8.429	
Slope gradient	<15°	0.07978	4.528	
	15°-25°	0.13023	7.392	
	25°-35°	0.23256	13.201	
	35°-45°	0.36040	20.458	
	45°-55°	0.45948	26.083	
	>55°	0.49914	28.334	
Slope aspect	N	0.12123	8.402	
	NE	0.22229	15.406	
	E	0.21689	15.032	
	SE	0.21675	15.022	
	S	0.19180	13.293	
	SW	0.15560	10.784	
	W	0.15511	10.750	
	NW	0.16316	11.308	

**Notes:** CV = Class value; HW = Hanging wall; F = Footwall

derived from peak ground motion amplitudes recorded on accelerometers, with interpolation based on both estimated amplitudes where data are lacking, and site amplification corrections (Dai et al. 2011). It is divided into six categories by 0.2 g intervals: <0.2 g, 0.2-0.4 g, 0.4-0.6 g, 0.6-0.8 g, 0.8-1.0 g and >1.0 g (Figure 9 (a)). The correlation between PGA and landslide distribution is shown in Table 1. The landslide density increases with

PGA and reaches the peak at the PGA value of 0.8-1.0 g. The landslide density is quite low when PAG is less than 0.2 g, but it increases rapidly within the range of 0.2–1.0 g.

#### 4.2 Distance from co-seismic fault

The co-seismic fault data layer was generated from a fault surface rupture map surveyed by the

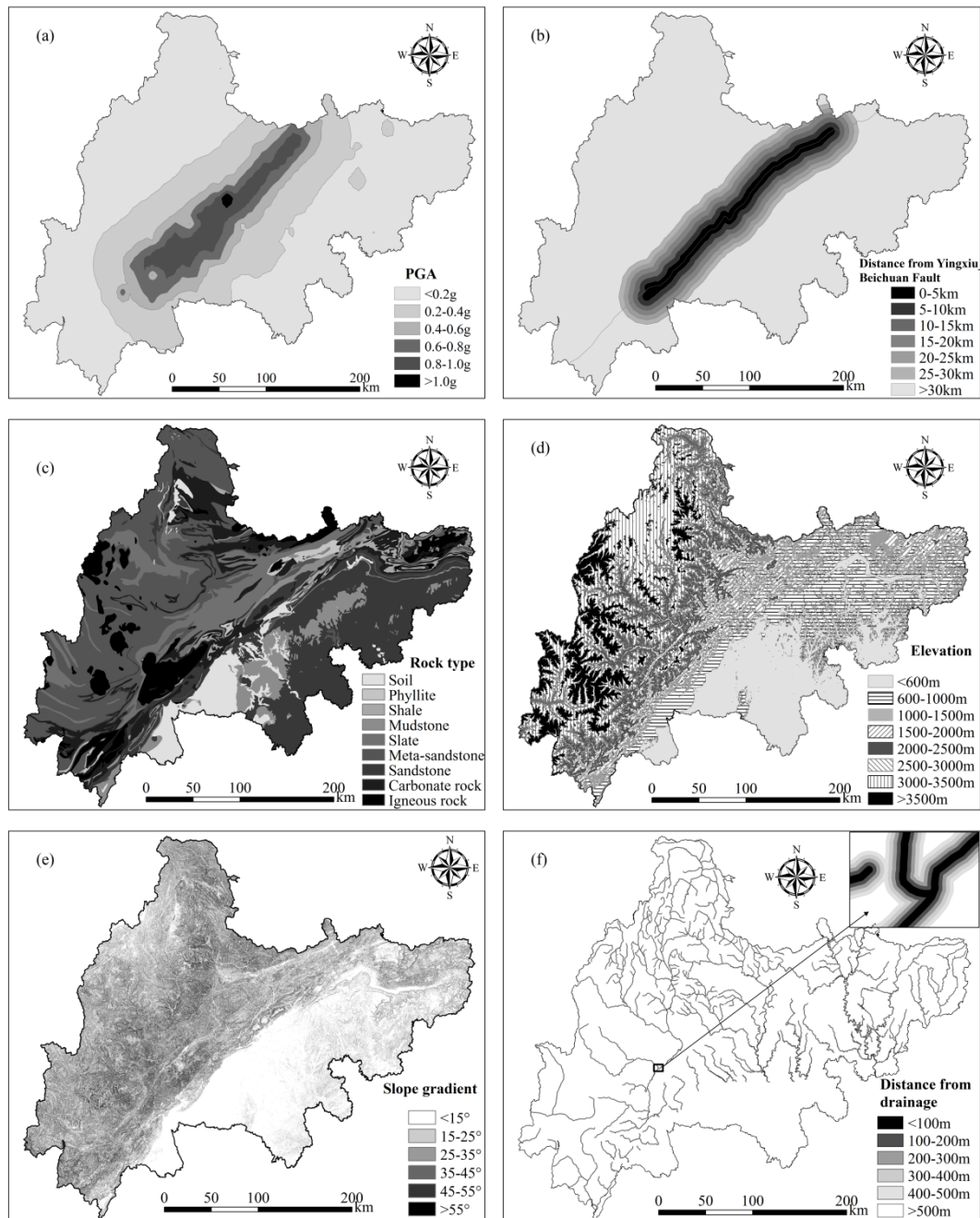


**Figure 9** The influencing parameters of co-seismic landslides. (a)PGA map, (b) Fault buffer map, (c) Lithology map, (d) Elevation map, (e) Slope gradient map, (f) Drainage buffer map

China Earthquake Administration. Given the significant hanging wall effect of the distribution of landslides triggered by Wenchuan earthquake (Huang and Li 2009a,b), the distance from co-seismic fault data layer was divided into seven classes by 5 km intervals on the hanging wall and the footwall respectively (Figure 9(b)). The correlation between the distance from co-seismic fault rupture and landslide is shown in Table 1. We can conclude that the landslide density decreases rapidly with the distance from co-seismic fault rupture on both the hanging wall and the footwall. It has the highest landslide density within 5 km to the rupture on the hanging wall, which is as high as 2.5 landslides per km<sup>2</sup>, almost double the density in the region of 5-10 km far from the rupture. 80% of the large-scale landslides (surface area > 50,000 m<sup>2</sup>) are located within a distance of 5 km from the rupture on the hanging wall. The landslide density within 5 km on the foot wall is almost the same as that of 10-15 km from the rupture on the hanging wall.

### 4.3 Lithology

The lithology data layer was generated from 1:250,000 digital geological maps. Based on lithological similarities, the rock types were grouped into 9 classes: igneous rock, carbonate rock, sandstone, meta-sandstone, slate, mudstone, shale, phyllite and soil (Figure 9(c)). The correlation between rock type and landslide distribution is shown in Table 1. The highest landslide concentration appeared in igneous rocks, while landslides in soil are rare. Field investigation revealed that the lithology plays an important role in determining landslide types, deep-seated slides were mainly distributed in strongly weathered and fractured sandstone and shale, large scale rock avalanche were mostly distributed in the rocks with rigid rocks (such as carbonate rocks) on the top and soft rocks (such as mudstone) on the underside, while shallow slides in phyllite, limestone and igneous rock are more common (Huang and Li 2009, Gorum et al. 2011).

### 4.4 Elevation

The surface topography is an important influencing factor of landslide distribution. Three

topographic parameters, including elevation, slope angle and slope aspect were selected to correlate with landslide distribution, which are derived from a 25 m × 25 m DEM generated from 1: 50,000 topographic maps. The elevation layer was classified into eight classes: <600 m, 600-1,000 m, 1,000-1,500 m, 1,500-2,000 m, 2,000-2,500 m, 2,500-3,000 m, 3,000-3,500 m and >3,500 m (Figure 9(d)). The correlation between elevation and landslide is shown in Table 1. The landslide density increase with the slope elevation until the maximum is reached in the 1,500-2,000 m and then decrease.

Field investigation suggested that an elevation of around 1,500 m a.s.l. corresponded to the position through which the broad valley developed into a canyon, with steep slopes. Above the elevation of 1,500 m the slope is generally gentle, and with elevation lower than 1,500 m, the slope turns quite steep. As a consequence of this rapid incision, there has been a fast unloading of the rock mass such that with stress release, the shaking related to the fault movement creates slope failures easily (Huang and Li 2009a,b).

### 4.5 Slope gradient

Slope gradient is an essential controlling factor of landslides and it is considered as one of the most important parameters for landslide susceptibility mapping. As slope gradient increases, the level of gravity induced shear stress in the slope increases; therefore, steeper hillslopes are expected to be prone to landsliding (Dai et al., 2011). The slope gradient layer is derived from the 25×25m DEM and classified into six classes: <15°, 15°-25°, 25°-35°, 35°-45°, 45°-55° and >55°(Figure 9(e)). The correlation between slope gradient and landslide distribution is shown in Table 1. The landslide density increases with slope gradient. Gentler hillslopes with a slope gradient of less than 15° have a negligible landslide density.

### 4.6 Slope aspect

Slope aspect related factors such as exposure to sunlight, land use, drying winds, soil saturation, and discontinuities may control the occurrence of landslides (Yalcin 2008). It is also often used to analyze the distribution rules of landslides

triggered by earthquake. In this study, aspect is divided into nine classes for the study area, namely, flat, N, NE, E, SE, S, SW, W, and NW. The correlations between slope aspect and landslide is shown in Table 1. The statistical result indicates that landslides triggered by the Wenchuan Earthquake is evenly distributed in eight slope aspects, and it has a slightly higher value in NE, E and SE direction than any others (see Table 1), which maybe indicates that slope aspect has minor influence on the distribution of the landslides triggered by the earthquake.

#### 4.7 Distance to drainage

Except the significant hanging wall effect, the landslides triggered by the Wenchuan earthquake show the feature of linear distribution along the drainage lines (Huang and Li 2009a, b). The undercutting action of the drainage may trigger instability of slopes. Along the drainage most landslides occur due to the slope undercutting during a high discharge condition and its effect decreases with the increase in the distance from the drainage lines. Thus, distance of a landslide from drainages was considered as a controlling factor of earthquake triggered landslides. The distance to main drainage lines was generated from the drainage network obtained from the digital topographic map, grouped into six classes by 100m intervals: 0-100m, 100-200 m, 200-300 m, 300-400 m, 400-500 m and >500 m (Figure (f)). The relationship between landslide and distance from drainage line is shown in Table 1. As the distance from a drainage line increases, the landslide density first increases and then decreases and the maximum is reached at a distance of 200-400 m. This could be attributed to the fact that terrain modification caused by gully erosion and undercutting may influence the slope stability (Lee and Talib 2005).

## 5 Landslide Susceptibility Mapping

### 5.1 Training samples

An important issue in the use of multi-variate statistical analysis is the number of training samples that should be taken to create the

independent variable for the LR analysis. Generally, it is recommended to use equal proportions of 1 (landslide) and 0 (no-landslide) pixels in LR, but there are different opinions among researchers (Ayalew and Yamagishi 2005). Some researchers used all data with an unequal proportion of landslide and non-landslide pixels (Ohlmacher and Davis 2003; Ayalew and Yamagishi 2005). This method was mostly adopted when the number of landslides are relatively small. If the study area is large and the landslide inventory contains many landslides there, a huge volume of data needs to be included in this method. Some authors used the total landslide pixels and randomly selected an equal number of no-landslide pixels from the landslide free areas (Yesilnacar and Topal 2005). Other researchers only used the data of part of the study area under investigation to calculate the LR coefficients (Atkinson and Massari 1998; Dai and Lee 2002). In this study, 3,000 landslide pixels were chosen from the source area of the inventoried landslides and an equal number of non-landslides pixels were randomly chosen for landslide free area for LR analysis in this study. By means of cross tabulating the sample map with each of the influencing parameter maps, a table has been created containing 8 columns with landslide status (1 or 0) and the class values of each parameter at the corresponding sample location.

### 5.2 Statistical results of LR

The table was then used as input into a binomial LR model using the statistical software of SPSS to calculate the coefficient of each influencing parameter. The method of forward stepwise regression (Likelihood Ratio) was adopted for variables choosing. In this approach, one adds variables to the model one at a time. At each step, each variable that is not already in the model is tested for inclusion in the model. The most significant of these variables is added to the model, so long as its P-value is below some pre-set level. It is customary to set this value at 0.1, because of the exploratory nature of this method. 6 independent parameters including distance from co-seismic fault, slope gradient, lithology, elevation, distance from drainage and PGA were added into the final LR model. The results indicated that the distance from co-seismic fault was the most significant

parameter followed by slope gradient and PGA. Aspect was excluded, because its P-value was 0.266 which was larger than the threshold of 0.1. The final logistic regression model was based on the variables presented in Table 2. In this study, all coefficients are positive except the intercept (Table 2), indicating that they are positively related to the probability of landslide formation. As shown in Table 3, 667 observed landslide pixels and 707 non-landslide pixel among the training samples were not predicted correctly. The overall accuracy of the sampling dataset is 77.1% and it is acceptable (Süzen and Doyuran 2003).

**Table 2** The regression coefficients obtained for the six independent parameters

Independent parameter	Coefficient
Intercept	-3.784
Slope gradient	9.165
Distance from co-seismic fault	12.585
Lithology	6.173
Elevation	3.662
PGA	0.710
Distance from drainage	6.364
Aspect	/

**Table 3** Classification table of training samples (The cut value is 0.5)

Observed	Predicted		Percentage correct
	1	0	
1	2,333	667	77.8
0	707	2,293	76.4
Total			77.1

**Notes:** 1=Landslide; 0=Non-landslide

**Table 4** Summary statistics of logistic regression (LR) model

Statistics	Value
Total number of pixels	6,000
-2ln L(L = likelihood)	5,561.234
Model chi-square( $\chi^2$ )	2,756.532
Cox & Snell R <sup>2</sup>	0.368
Nagelkerke R <sup>2</sup>	0.491

The summary statistics of the regression conducted in this study are shown in Table 4. The value of model chi-square ( $\chi^2$ ) provides the usual significance test for LR. The high value of model chi-square indicates that the occurrence of landslides is far less likely under the null hypothesis (without landslide influencing parameters) than the full regression model. The

value of model chi-square is quite high to conclude that the selected independent parameters in this study have a great influence on the occurrence of co-seismic landslides. The pseudo R<sup>2</sup> value cautiously indicates how the LR model fits the dataset and a pseudo R<sup>2</sup> greater than 0.2 shows a relatively good fit in landslide susceptibility mapping (Ayalew and Yamagishi 2005). Two pseudo R<sup>2</sup> values of Cox & Snell and Nagelkerke were obtained with Hosmer-Lemeshow test in this study (Table 4). They both are greater than 0.2 which indicates a reasonable fit to the sample date.

### 5.3 Susceptibility mapping

With the logistic regression coefficients, the probability of landslide occurrence (*P*) was calculated with Equation (4) using the raster calculator tool of ArcGIS 9.3.

$$P = 1/1+M \tag{4}$$

$$M = e^{3.784-(9.165*Slope\ gradient)-(12.585*Distance\ from\ co-seismic\ fault)-(6.173*Lithology)-(3.662*Elevation)-(0.710*PGA)-(6.364*Distance\ from\ drainage)} \tag{5}$$

LR give predictions of landslides probability (0~1) instead of directly predicting the presence or absence of landslide. The evaluation can be done with respect to another dataset in the same area or framework or could be tested in an adjacent area of similar geo-environmental conditions to find out the reliability (Ayalew and Yamagishi 2005). In this case, we use the so-called Relative Operating Characteristic (ROC) to carry out the accuracy assessment for the result of LR model. The input for the ROC curve analysis is a table which contains the predicted probabilities of the samples chosen for the purpose of accuracy assessment and their actual state of the dependent variable represented as 1(present) and 0 (absent). The ROC value ranges from 0.5 to 1, where 1 indicates a perfect fit and 0.5 represents a random fit. 8,869 landslide pixels and 9,924 non-landslide pixels were chosen randomly for the accuracy assessment for the result of LR model. A value of 0.806 is obtained in this study (Figure 10), which can be taken as a sign of acceptable correlation between the independent and dependent variables.

To generate a susceptibility map, the method adopted in literature is to divide the histogram of the probability map into different categories based

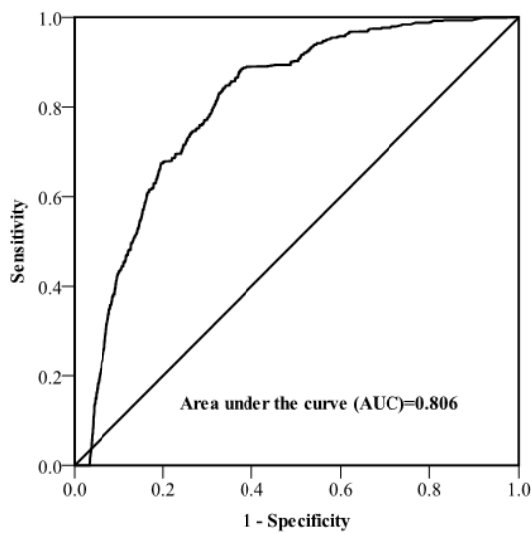


**Figure 10** Area under curve (AUC=0.806) representing the prediction rate of the LR model

**Table 5** The classification system used to produce landslide susceptibility map

Probability	Class	Coverage (%)	Landslide (%)
0-0.0653	Very low	80.4	2.3
0.0653-0.1932	Low	11.6	6.7
0.1932-0.3791	Medium	4.2	17.7
0.3791-0.6425	High	2.3	28.1
0.6425-1	Very high	1.6	45.2

on expert opinions. This type of changing continuous data into two or more categories does not take into account the relative position of a case within the probability map and is neither fully automated nor statistically tested (Lulseged and Hiromitsu 2005). In this study, we considered three classification systems that use natural breaks, equal intervals and standard deviations, and attempted to choose the one that best fits our investigation information. A few trials showed that natural breaks classification system is the best one. The susceptibility map was then reclassified into five categories of landslide susceptibility (very low, low, medium, high and very high). The class boundaries were as follows: 0-0.0653 very low susceptibility, 0.0653-0.1932 low susceptibility, 0.1932-0.3791 medium susceptibility, 0.3791-0.6425 high susceptibility and 0.6425-1 very high susceptibility (Table 5).

As shown in Table 3 and Figure 11, 92.0% of the study area is designated to be low and very low susceptible with corresponding 9.0% of the total inventoried landslides. Medium susceptible zones

make up 4.2% of the area with 17.7% of the total landslides. The rest of the area was classified as high and very high susceptibility that make up 3.9% of the area with corresponding 73.3% of the total landslides.

## 6 Discussions

### 6.1 Why PGA is not as significant as expected to the occurrence of co-seismic landslides?

Theoretically speaking, the distribution density of co-seismic landslide become higher when PGA become larger, so PGA should be one of the factors determining spatial distribution of landslides triggered by the earthquake. However, our analysis suggested that PGA is the least significant factor. Observing from Table 1, when PGA was lower than 1.0 g, the landslide density increased with the increase of PGA, but when PGA is higher than 1.0 g, the landslide density decreased dramatically. From Figure 9(a), it can be discovered that the area with PGA being higher than 1.0 g is very small and near the Beichuan city. Dai et al. (2011) obtained similar results with ours, as shown in Figure 12. The PGA data acquired from the USGS website is derived from far-distance ground-motion station, thus the data has low accuracy, which may be the main reason accounting for the low correlation between PGA and the distribution of landslides when PGA is greater than 1.0 g. If the higher resolution PGA data is adopted, the significance should increase a lot.

### 6.2 Does slope aspect influence the occurrence of co-seismic landslides?

Slope aspect is often used to analyze the distribution of landslides triggered by earthquake, but according to our statistical analysis, the landslides are well distributed in each slope direction, as shown in Table 1. Aspect was excluded from the independent parameters for LR in this study. However we discovered that landslides were easier to happen in the slopes of certain direction in some special regions during the process of remote-sensing interpretation. As shown in Figure 13, there were more landslides in the slopes

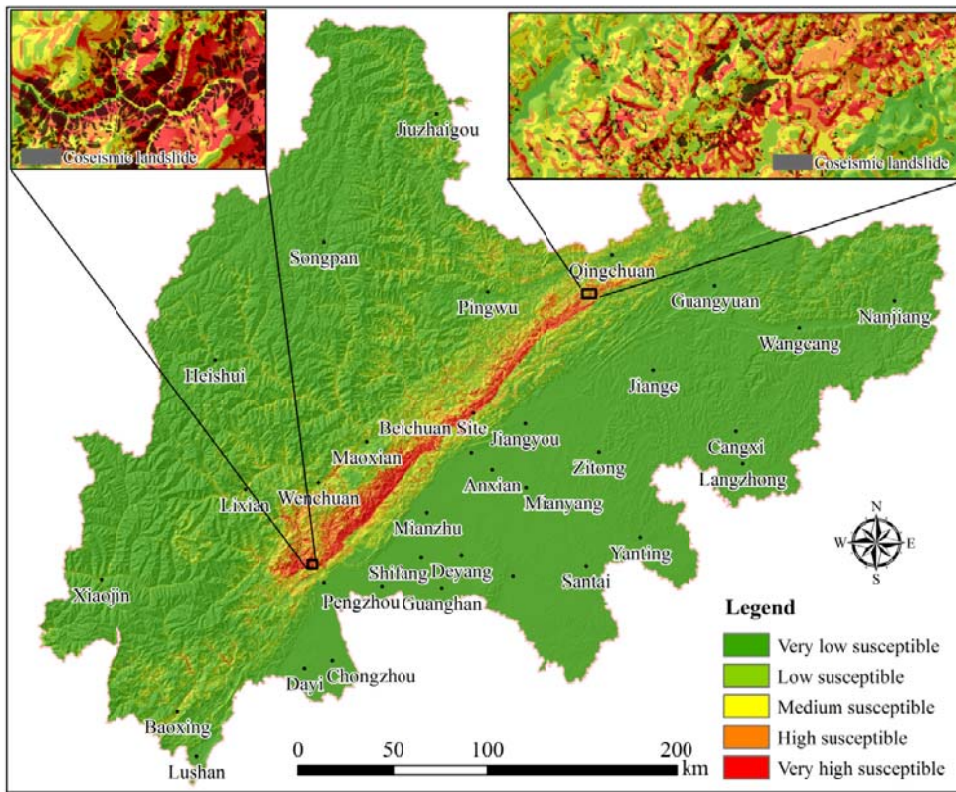


**Figure 11** Landslide susceptibility map of the Wenchuan earthquake disaster area

backing towards the spreading direction of seismic wave than in the slopes facing the spreading direction of seismic wave. Xu and Li (2011) named this phenomenon “back-slope effect”, and assumed that this effect is related with micro-landform and the spreading direction of seismic waves.

### 7 Conclusions

The paper proposed a logistic regression model combined with BSA for landslide susceptibility mapping in the Wenchuan earthquake area. A landslide database including 43,842 landslides with a total area of 632 km<sup>2</sup>, was developed by interpretation of multi-temporal and

multi-resolution remote sensing images. The landslides can be classified into three major categories: swallow, disrupted slides and falls; deep-seated slides and falls and rock avalanches from remote sensing images.

The landslides were highly concentrated in certain areas with special geologic and geomorphic settings. The correlation between landslides distribution and the influencing parameters including distance from co-seismic fault, lithology,

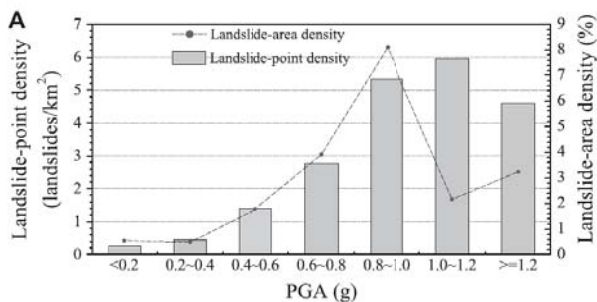


**Figure 12** Landslide density vs. PGA (Dai et al. 2011)

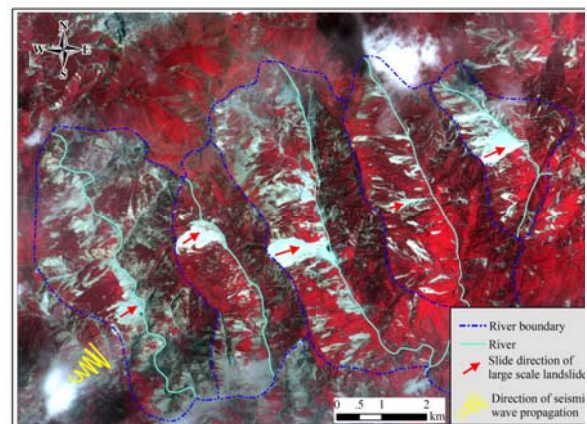


**Figure 13** The ALOS image showing the “back-slope effect” of landslides induced by the Wenchuan earthquake

slope gradient, elevation, PGA and distance from drainage, were analyzed by GIS tools. The result indicated that distance from co-seismic fault was the most significant parameter followed by slope gradient and PGA was the most insignificant one. Although slope aspect was excluded from the independent parameters for LR, it has a significant effect on the occurrence of co-seismic landslides in some areas.

The study area was classified into five categories of landslide susceptibility: very low, low, medium, high and very high. 92.0% of the study area belongs to low and very low susceptible with corresponding 9.0% of the total inventoried landslides. Medium susceptible zones make up 4.2% of the area with 17.7% of the total landslides. The rest of the area was classified as high and very high susceptibility that make up 3.9% of the area with corresponding 73.3% of the total landslides. The landslide susceptibility mapping in this study is event-based. Although the susceptibility map may make no sense to predict the distribution of landslides triggered by the future earthquake events in this region, it can reveal the likelihood of

future landslides and debris flows, and it will be useful for planners during the rebuilding process and for future zoning issues.

## Acknowledgments

This study is financially supported by the National Key Technology R&D Program (Grant No. 2011BAK12B01), the Young Foundation of National Natural Science of China (Grant No.41202210), the Education Department Innovation Research Team Program (Grant No.IRT0812) and the Young Foundation of Chengdu University of Technology and the Education Department of Sichuan Province (Grant Nos.2010QJ15 and 11ZB262). We appreciate that Prof. Liu Jianguo from Imperial College London, United Kingdom, the Bureau of Land and Resources and the Bureau of Surveying and Mapping of Sichuan Province and Japan Aerospace Exploration Agency (JAXA) for providing the data for our research. The editor and three anonymous reviewers provided many critical comments which are gratefully appreciated.

## References

- Aleotti P, Chowdhury R (1999) Landslide hazard assessment: summary review and new perspectives. *Bulletin of Engineering Geology and the Environment* 58(1): 21-44. DOI: 10.1007/s100640050066
- Ayalew L, Yamagishi H (2005) The application of GIS-based logistic regression for landslide susceptibility mapping in the Kakuda-Yahiko Mountains, Central Japan. *Geomorphology* 65(1-2): 15-31. DOI: 10.1016/j.geomorph.2004.06.010
- Aykut (2012) A comparison of landslide susceptibility maps produced by logistic regression, multi-criteria decision, and likelihood ratio methods: a case study at İzmir, Turkey. *Landslide* 9(1): 93-106. DOI: 10.1007/s10346-011-0283-7
- Bai SB, Wang J, Lv GN, et al. (2010) GIS-based logistic regression for landslide susceptibility mapping of the Zhongxian segment in the Three Gorges area, China. *Geomorphology* 115: 23-31. DOI: 10.1016/j.geomorph.2009.09.025
- Chen ZH, Wang JF (2007) Landslide hazard mapping using logistic regression model in Mackenzie Valley, Canada. *Nat Hazards* 42(1): 75-89. DOI: 10.1007/s11069-006-9061-6
- Dai FC, Xu C, Yao X, et al. (2011) Spatial distribution of landslides triggered by the 2008 Ms 8.0 Wenchuan earthquake, China. *Journal of Asian Earth Sciences* 40(4): 883-895. DOI: 10.1016/j.jseaes.2010.04.010
- Das I, Sahoo S, Westen CV, et al. (2010) Landslide susceptibility assessment using logistic regression and its comparison with a rock mass classification system, along a road section in the northern Himalayas (India). *Geomorphology* 114: 627-637. DOI: 10.1016/j.geomorph.2009.09.023
- Das I, Stein A, Kerle N, et al. (2012) Landslide susceptibility mapping along road corridors in the Indian Himalayas using Bayesian logistic regression models. *Geomorphology* 179: 116-125. DOI: 10.1016/j.geomorph.2012.08.004
- Dong JJ, Tung YH, Chen CC, et al. (2011) Logistic regression model for predicting the failure probability of a landslide dam. *Engineering Geology* 117: 52-61. DOI: 10.1016/j.enggeo.2010.10.004
- Douglas J (2003) Earthquake ground motion estimation using strong-motion records: a review of equations for the estimation of peak ground acceleration and response spectral ordinates. *Earth-Science Reviews* 61:43-104. DOI: 10.1016/S0012-8252(02)00112-5
- Gorum T, Fan XM, Westen CJ, et al. (2011) Distribution pattern of earthquake-induced landslides triggered by the 12 May 2008 Wenchuan earthquake. *Geomorphology* 133(3-4): 152-167. DOI: 10.1016/j.geomorph.2010.12.030
- Guzzetti F, Mondini AC, Cardinali M, et al. (2012) Landslide inventory maps: New tools for an old problem. *Earth-Science Reviews* 112(1-2): 42-66. DOI: 10.1016/j.earscirev.2012.02.001
- Huang RQ, Li WL (2009a) Analysis of the geo-hazards triggered by the 12 May 2008 Wenchuan Earthquake, China. *Bull of Engineering Geology and the Environment* 68: 363-371. DOI: 10.1007/s10064-009-0207-0
- Huang RQ, Li WL (2009b) Development and distribution of geohazards triggered by the 5.12 Wenchuan Earthquake in China. *Science in China Series E-Technological Sciences* 52(4): 810-819. DOI: 10.1007/s11431-009-0117-1
- Huang RQ, Pei XJ, Li TB (2008) Basic characteristics and formation mechanism of the largest scale landslide at

- Daguangbao occurred during the Wenchuan earthquake. *Journal of Engineering Geology* 16(6): 730-741. (In Chinese)
- Huang RQ, Xu Q, Huo JJ (2011) Mechanism and geo-mechanics models of landslides triggered by 5.12 Wenchuan earthquake. *Journal of Mountain Science* 8: 200-210. DOI: 10.1007/s11629-011-2104-9
- Keefer DK (1984) Landslides caused by earthquakes. *Geological Society of America Bulletin* 95: 406-421. DOI: 10.1130/0016-7606
- Lulseged A, Hiromitsu Y (2005) The application of GIS-based logistic regression for landslide susceptibility mapping in the Kakuda-Yahiko Mountains, Central Japan. *Geomorphology* 65(1-2):15-31. DOI: 10.1016/j.geomorph.2004.06.010
- Parker RN, Densmore AL, Rosser NJ, et al. (2011) Mass wasting triggered by the 2008 Wenchuan earthquake is greater than orogenic growth. *Nature Geoscience* 4: 449-452. DOI: 10.1038/NNGEO1154
- Qi SW, Xu Q, Lan HX, et al. (2010) Spatial distribution analysis of landslides triggered by 2008.5.12 Wenchuan Earthquake, China. *Engineering Geology* 116: 95-108. DOI: 10.1016/j.enggeo.2010.07.011
- Qi SW, Xu Q, Lan HX, et al. (2012) Resonance effect existence or not for landslides triggered by 2008 Wenchuan earthquake: A reply to the comment by Drs. Xu Chong and Xu Xiwei. *Engineering Geology* 151:128-130. DOI: 10.1016/j.enggeo.2012.08.003
- Soeters R, Westen CJ (1996) Slope instability recognition, analysis, and zonation. In Turner, K.A. & Schuster, R.L. (eds), *Landslides: investigation and mitigation* 247:129-177. Washington, D.C.: Transport Research Board.
- Song YQ, Gong JH, Gao S, et al. (2012) Susceptibility assessment of earthquake-induced landslides using Bayesian network: A case study in Beichuan, China. *Computers & Geosciences* 42:189-199. DOI: 10.1016/j.cageo.2011.09.011
- Su FH, Cui P, Zhang JQ et al. (2010) Susceptibility Assessment of Landslides Caused by the Wenchuan Earthquake Using a Logistic Regression Model. *Journal of Mountain Science* 7(3): 234-245. DOI: 10.1007/s11629-010-2015-1
- Süzen ML, Doyuran V (2003) A comparison of the GIS based landslide susceptibility assessment methods: multivariate versus bivariate. *Environmental Geology* 45(5):665-679. DOI: 10.1007/s00254-003-0917-8
- Tang C, Zhu J, Li WL, et al. (2009) Rainfall-triggered debris flows following the Wenchuan earthquake. *Bull Eng Geol Environ* 68: 187-194. DOI: 10.1007/s10064-009-0201-6
- Tom P, Chen J, Eric K (2008) Stress changes from the 2008 Wenchuan earthquake and increased hazard in the Sichuan basin. *Nature* 454: 509-510. DOI: 10.1038/nature07177
- Van Western CJ, Castellanos E, Kuriakose SL (2008) Spatial data for landslide susceptibility, hazard, and vulnerability assessment: An overview. *Engineering Geology* 102(3-4): 112-131. DOI: 10.1016/j.enggeo.2008.03.010
- Varnes DJ (1984) *Landslide hazard zonation: a review of principles and practice*. Paris: UNESCO Press.
- Wang FW, Chen QG, Lynn H, et al. (2009) Preliminary investigation of some large landslides triggered by the 2008 Wenchuan earthquake, Sichuan Province, China. *Landslides* 6(1): 47-54. DOI: 10.1007/s10346-009-0141-z
- Xu C, Dai FC, Xu XW, et al. (2012c) GIS-based support vector machine modeling of earthquake-triggered landslide susceptibility in the Jianjiang River watershed, China. *Geomorphology* 145-146: 70-80. DOI: 10.1016/j.geomorph.2011.12.040
- Xu C, Xu XW, Dai FC, et al. (2012a) Comparison of different models for susceptibility mapping of earthquake triggered landslides related with the 2008 Wenchuan earthquake in China. *Computers & Geosciences* 46: 317-329. DOI: 10.1016/j.cageo.2012.01.002
- Xu C, Xu XW, Dai FC, et al. (2012b) Landslide hazard mapping using GIS and weight of evidence model in Qingshui River watershed of 2008 Wenchuan Earthquake struck Region. *Journal of Earth Science* 23(1): 97-120. DOI: 10.1007/s12583-012-0236-7
- Xu Q, Li WL (2011). Study on the direction effects of landslides triggered by Wenchuan Earthquake. *Journal of Sichuan University (Engineering Science Edition)* 42(S1): 7-14. (In Chinese)
- Xu Q, Zhang S, Li WL (2011) Spatial Distribution of Large-scale Landslides Induced by the Wenchuan Earthquake. *Journal of Mountain Science* 8: 246-260. DOI: 10.1007/s11629-011-2105-8
- Yalcin A (2008) GIS-based landslide susceptibility mapping using analytical hierarchy process and bivariate statistics in Ardesen (Turkey): comparisons of results and confirmations. *Catena* 72 (1):1-12. DOI: 10.1016/j.catena.2007.01.003
- Yin YP, Wang FW, Sun P (2009) Landslide hazards triggered by the 2008 Wenchuan earthquake, Sichuan, China. *Landslides* 6:139-151. DOI: 10.1007/s10346-009-0148-5
- Youd TL, Perkins DM (1978) Mapping liquefaction-induced ground failure potential. *Journal of the Geotechnical Engineering Division* 104:433-446.